

**Conference Paper No: PF-01**

**Optimization of growth parameters of electrodeposited tin oxide thin films for PV applications**

F. S. B. Kafi<sup>1\*</sup>, B. H. Gunaratne<sup>1</sup>, K. M. D. C. Jayathilaka<sup>1</sup> and R. P. Wijesundera<sup>1</sup>

<sup>1</sup>Department of Physics and Electronics, University of Kelaniya, Sri Lanka  
kafi@kln.ac.lk\*

**Abstract**

Tin oxide (SnO<sub>2</sub>) is a promising photoactive semiconducting material due to its optoelectronics properties. Even though, growth of SnO<sub>2</sub> using the method of electrodeposition is advantageous, it has paved low attention among semiconductor researchers. In this study, well-adhered photoactive SnO<sub>2</sub> thin film was successfully electrodeposited on Cu substrates. The growth parameters, such as film deposition potential, bath temperature, and duration of deposition were optimized. Electrodeposition of SnO<sub>2</sub> layers was performed on copper substrates in a three-electrode electrochemical cell using a solution containing 30 mM SnCl<sub>2</sub> and 150 mM HNO<sub>3</sub> at a deposition potential of -0.85 V vs. Ag/AgCl. The fabricated best thin film resulted J<sub>SC</sub> value of 410  $\mu\text{A cm}^{-2}$  and V<sub>OC</sub> value of 113 mV in 0.1 M NaNO<sub>3</sub> electrolyte. The best thin film obtained at a bath temperature of 85°C for a deposition time of 120 seconds. The Mott-Schottky analysis revealed that the fabricated SnO<sub>2</sub> thin film exhibits n-type conductivity, and it has a flat band potential of -0.51 V vs. Ag/AgCl.

**Keywords**

Electrodeposition, Photovoltaics, SnO<sub>2</sub>, Thin film, Tin oxide

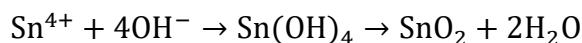
**Introduction**

Tin oxide (SnO<sub>2</sub>) is considered to be a defect type photoactive semiconducting material. It has wide direct band gap of approximately 3.8 eV (Li et al., 2009). SnO<sub>2</sub> exhibits properties such as high mobility, excellent conductivity, great thermal stability and transparency in the visible region (Riahi et al., 2021). These properties are highly favorable for semiconductor applications. SnO<sub>2</sub> is already being using in solar cells (Xiong et al., 2018) as window layer as well as anode material for Li-ion batteries (J. S. Chen & Lou, 2013) and gas sensors (Das & Jayaraman, 2014).

Like all other metal oxide semiconductors (Kafi et al., 2020), SnO<sub>2</sub> thin films can be grown using techniques including chemical bath deposition (Khallaf et al., 2012), spray pyrolysis (Gordillo et al., 1994), sol-gel process (Chatelon et al., 1994), metal-organic deposition (Park et al., 2006), liquid flow deposition (Supothina, 2003) and electrodeposition (X. Chen et al., 2010). Among the range of techniques available for depositing SnO<sub>2</sub>, fabrication of SnO<sub>2</sub> using the method of electrodeposition is less reported in literature. Additionally, the fabrication of SnO<sub>2</sub> using the method of electrodeposition owes advantages like cost effectiveness, easiness, and uniformity in growth of thin film layer.

Electrodeposition of SnO<sub>2</sub> thin films requires the presence of hydroxyl ions (OH<sup>-</sup>) or O<sup>-</sup> radicals on or near the working electrode (Therese & Kamath, 2000). Various types of oxygen precursors can be utilized for this purpose, including hydrogen peroxide

(Pauporté & Lincot, 2001), nitrate ions (Izaki & Omi, 1997), and blown oxygen (Peulon & Lincot, 1998). Generally, application of a potential to the working electrode causes a reduction of the oxygen precursor resulting creation of OH<sup>-</sup> groups. Then, these anions create tin hydroxide (Sn(OH)<sub>4</sub>) using the Sn<sup>4+</sup> ions in the solution of SnO<sub>2</sub> film deposition bath. However, this Sn(OH)<sub>4</sub> is unstable. Thus, it quickly dehydrates and precipitates to form SnO<sub>2</sub>, as presented in the following reaction:



Many researchers have developed various film deposition baths for the fabrication of SnO<sub>2</sub> thin film employing electrodeposition technique is listed in the Table 1.

**Table 1.** Reported film deposition baths for fabrication of SnO<sub>2</sub> thin films

Working Electrode	Film deposition bath	Mode	References
Cu	20 mM SnCl <sub>2</sub> .2H <sub>2</sub> O 100 mM NaNO <sub>3</sub> 75 mM HNO <sub>3</sub>	Galvanostatically	(Chang et al., 2002)
Cu	25 mM SnCl <sub>2</sub> .2H <sub>2</sub> O 150 mM HNO <sub>3</sub>	Galvanostatically	(Chang et al., 2004)
Au	25 mM SnCl <sub>2</sub> .2H <sub>2</sub> O 100 mM NaNO <sub>3</sub> 75 mM HNO <sub>3</sub>	Potentiostatically	(Lai et al., 2006)
Pt	100 mM SnCl <sub>2</sub> .2H <sub>2</sub> O 400 mM NaNO <sub>3</sub> 500 mM HNO <sub>3</sub> 0.2 wt.% SDS	Potentiostatically	(Spray & Choi, 2007)
ITO	20 mM SnCl <sub>2</sub> .2H <sub>2</sub> O 100 mM NaNO <sub>3</sub> 75 mM HNO <sub>3</sub> 5 mM SDS	Potentiostatically	(Ishizaki et al., 2009)
Cu	20 mM SnCl <sub>4</sub> .5H <sub>2</sub> O 80 mM HNO <sub>3</sub>	Potentiostatically	(X. Chen et al., 2010)
ITO	30 mM SnSO <sub>4</sub> 1.07M HNO <sub>3</sub>	Potentiostatically	(Vequizo et al., 2010)
Cu	100 mM SnCl <sub>2</sub> .2H <sub>2</sub> O 500 mM NaNO <sub>3</sub> 400 mM HNO <sub>3</sub>	Potentiostatically	(Kim, S., Lee, H., Park, C. M., & Jung, 2012)

ITO	40 mM SnCl <sub>2</sub> 100 mM HNO <sub>3</sub> 100 mM NaNO <sub>3</sub>	Potentiostatically	(Daideche, K., Azizi, 2017)
-----	--	--------------------	-----------------------------

In this study, nitrate ion-based bath was used for the potentiostatically electrodeposition of the SnO<sub>2</sub> thin film followed by a pre-treatment of oxygen bubbling to the film deposition bath. The growth parameters such as potential of film deposition, temperature of the bath and duration of the film deposition were altered in order to find the optimum growth parameters. In literature, details of optimization of growth parameter for the SnO<sub>2</sub> film deposition is rarely reported. Further, the performance of photoactive SnO<sub>2</sub> thin films in sodium nitrate electrolyte is not reported. Thus, this study is significant to understand the electrical properties of electrodeposited SnO<sub>2</sub> thin films.

### Methodology

SnO<sub>2</sub> thin films were potentiostatically electrodeposited on well-cleaned copper substrates using a Hokuto Denko Potentiostat / Galvanostat HAB-151 in a setup of three-electrode electrochemical cell. The aqueous film deposition bath consisted of 30 mM stannous chloride (SnCl<sub>2</sub> reagent grade, 98%) and 150 mM nitric acid (HNO<sub>3</sub> reagent grade, 69%). The working electrode was the copper foil and the counter electrode was a platinum foil. The reference electrode was a Ag/AgCl electrode. Initially, a pre-treatment step was carried out in order to oxidize the stannous ions (Sn<sup>2+</sup>) into stannic ions (Sn<sup>4+</sup>). Here, the oxygen gas was bubbled into the electrochemical bath for 1 hour at the relevant temperature of the electrodeposition bath. A cyclic voltammetry was taken to determine the deposition potential. Then, the growth parameters such as temperature of the film deposition bath and the duration of the film depositions were altered, in order to identify the optimum growth parameters. The tested temperature values of the film deposition bath were 70, 75, 80, 85, 90, 95 °C and the tested duration of the film deposition were 30, 60, 120, 150, 180, 240 seconds. After the SnO<sub>2</sub> thin film deposition, all the samples were washed with deionized water, then immersed in 0.1 M sodium nitrate (NaNO<sub>3</sub>) and dried under ambient conditions in a desiccator.

A solution containing 0.1 M NaNO<sub>3</sub> was used as the photoelectrochemical cell (PEC) for the SnO<sub>2</sub> thin film characterization. The current-voltage (I-V) and capacitance-voltage (C-V) characterizations were implemented through Gamry G series potentiostat/galvanostat/ ZRA instrument. The I-V characterization was conducted under illumination with a mercury lamp.

### Result and discussion

The Figure 1 depicts the cyclic voltammetry curve obtained using the Gamry instrument. From the curve of cyclic voltammogram shown in Figure 1, it is clear that well-defined cathodic peaks that can be observed around the potential values of -0.20 V and -0.77 V vs. Ag/AgCl. At the certain deposition potential value of -0.20 V vs. Ag/AgCl, no visible thin film was deposited on the working electrode. At the deposition potential value of -0.77 V vs. Ag/AgCl a thin film of SnO<sub>2</sub> was grown on the working electrode. However, the thin film formed at deposition potential value of -0.77 V vs. Ag/AgCl was not well-adhere to the substrate. Therefore, a set of samples was deposited across a range of potentials, varying from 0.60V to 0.90 V vs. Ag/AgCl. Thus, it is found that the best

adhered SnO<sub>2</sub> thin films were form at the deposition potential value of 0.85 V vs. Ag/AgCl.

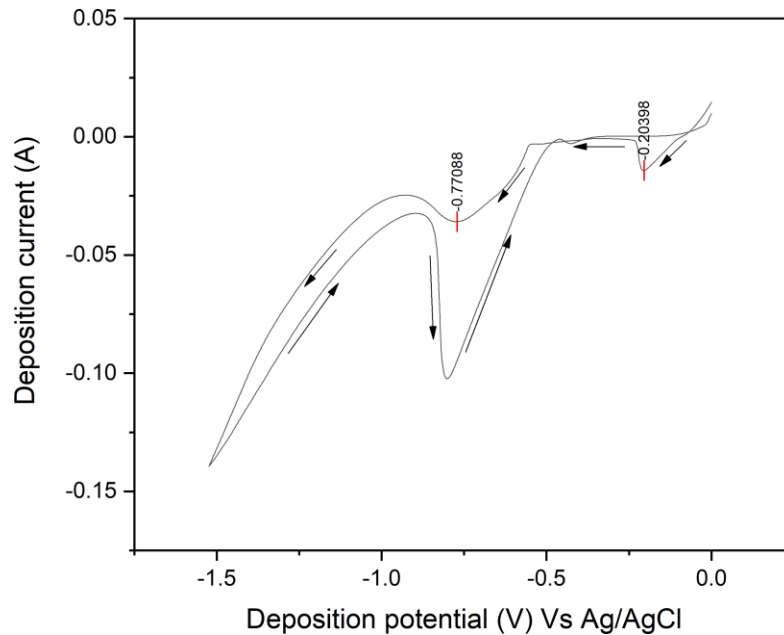


**Figure 1.** Cyclic voltammetric curve of SnO<sub>2</sub> thin film deposition

The Table 2 displays the values of short circuit current densities ( $J_{SC}$ ) and open circuit voltages ( $V_{OC}$ ) resulted for the SnO<sub>2</sub> thin films deposited at deposition potential value of -0.85 V vs. Ag/AgCl and at the bath temperature values of 80°C, 85°C, and 90°C. The photoresponses resulted for the other temperature values are insignificant.

**Table 2.**  $J_{SC}$  and  $V_{OC}$  values for the SnO<sub>2</sub> thin films deposited at different temperature values of film deposition for 120 seconds

Temperature (°C)	$J_{SC}$ ( $\mu\text{Acm}^{-2}$ )	$V_{OC}$ (mV)
80	309	69
85	410	113
90	91	50

The Table 3 displays the  $J_{SC}$  and  $V_{OC}$  values for the SnO<sub>2</sub> thin films deposited at deposition potential value of -0.85 V vs. Ag/AgCl and at the deposition durations of 60, 90, 120 and 150 seconds. The photoresponses resulted for the other deposition durations were insignificant.

The optimal photoactive performance was achieved from the films grown in a bath consisting of 30 mM SnCl<sub>2</sub> and 150 mM HNO<sub>3</sub> at a deposition potential of - 0.85 V vs. Ag/AgCl and bath temperature of 85 °C for a deposition duration of 120 seconds. Light modulated I-V curve for the optimum sample is shown in Figure 02. Here the area exposed for the I-V characterization was 25 mm<sup>2</sup>.

**Table 3.**  $J_{SC}$  and  $V_{OC}$  values for the  $\text{SnO}_2$  thin films deposited at different film deposition durations at the bath temperature value of  $85^\circ\text{C}$ .

Time (s)	$J_{SC}$ ( $\mu\text{Acm}^{-2}$ )	$V_{OC}$ (mV)
60	59	9
90	254	51
120	410	113
150	227	42

Figure 3 represents the Mott-Schottky plot which was obtain for the optimum sample. According to the Figure 3 it is clear that  $\text{SnO}_2$  film exhibits n-type conductivity and has a flat band potential of  $-0.51\text{ V}$  vs.  $\text{Ag}/\text{AgCl}$ .

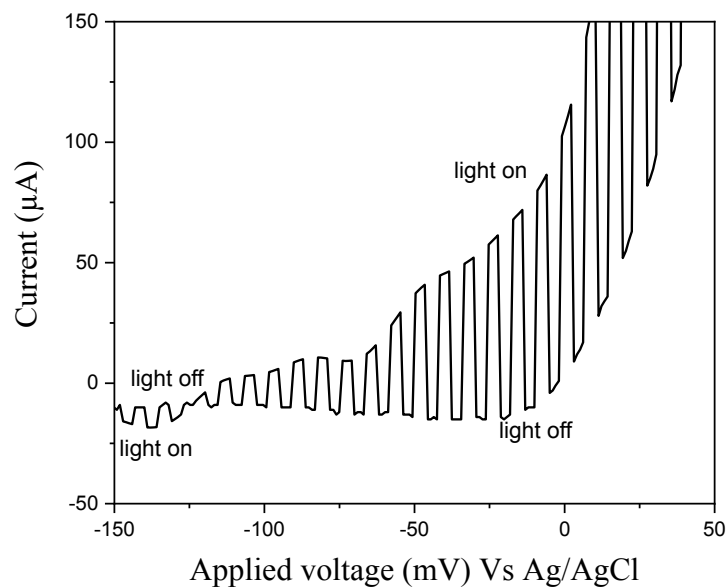


**Figure 2.** Dark and light current-voltage characteristics for the film deposited at optimum growth condition

### Conclusion

In this study, it is found that successfully photoactive n-type  $\text{SnO}_2$  thin films can be electrodeposited on  $\text{Cu}$  substrate. The best sample resulted the  $J_{SC}$  value of  $410\ \mu\text{Acm}^{-2}$  and  $V_{OC}$  value of  $113\text{ mV}$ . The quality photoactive samples can be deposited in a three electrochemical cell consisting of  $30\text{ mM SnCl}_2$  and  $150\text{ mM HNO}_3$  at  $-0.85\text{ V}$  vs.  $\text{Ag}/\text{AgCl}$  for  $120$  seconds and bath temperature of  $85^\circ\text{C}$ . Moreover, the flat band potential resulted for the best  $\text{SnO}_2$  thin films was  $-0.51\text{ V}$  vs.  $\text{Ag}/\text{AgCl}$ .

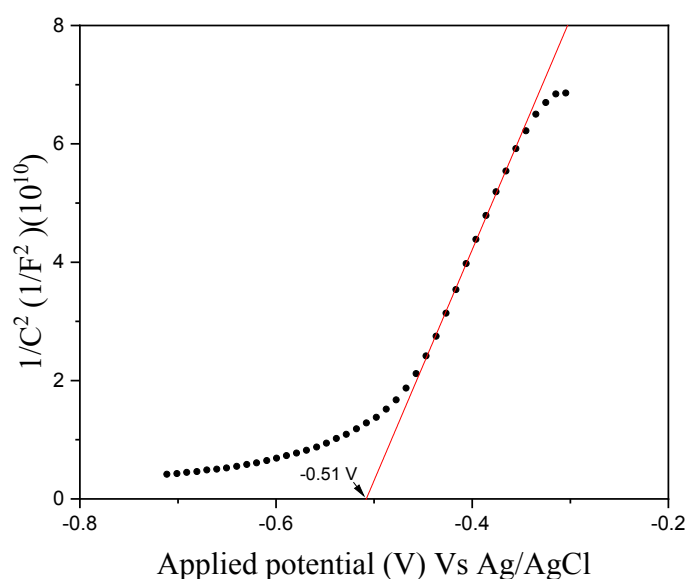


**Figure 3.** Mott–Schottky plot obtained in a PEC containing 0.1 M sodium nitrate aqueous solution for SnO<sub>2</sub> thin film electrodeposited under optimum growth conditions.

### Acknowledgment

This work was supported by Internal Research Grant, University of Kelaniya under the research grant no: RP/03/02/05/01/2022

### References

- Chang, S. T., Leu, I. C., & Hon, M. H. (2002). *Electrochemical and Solid-State Letters*, 5(8), C71. <https://doi.org/10.1149/1.1485808>
- Chang, S. T., Leu, I. C., Liao, C. L., Yen, J. H., & Hon, M. H. (2004). *Journal of Materials Chemistry*, 14(12), 1821–1826. <https://doi.org/10.1039/B316459D>
- Chatelon, J. P., Terrier, C., Bernstein, E., Berjoan, R., & Roger, J. A. (1994). *Thin Solid Films*, 247(2), 162–168. [https://doi.org/10.1016/0040-6090\(94\)90794-3](https://doi.org/10.1016/0040-6090(94)90794-3)
- Chen, J. S., & Lou, X. W. (David). (2013). *Small*, 9(11), 1877–1893. <https://doi.org/10.1002/sml.201202601>
- Chen, X., Liang, J., Zhou, Z., Duan, H., Li, B., & Yang, Q. (2010). *Materials Research Bulletin*, 45(12), 2006–2011. <https://doi.org/10.1016/j.materresbull.2010.07.029>
- Daideche, K., Azizi, A. (2017). *J Mater Sci: Mater Electron*, 28, 8051–8060. <https://doi.org/10.1007/s10854-017-6511-8>
- Das, S., & Jayaraman, V. (2014). *Progress in Materials Science*, 66, 112–255. <https://doi.org/10.1016/j.pmatsci.2014.06.003>
- Gordillo, G., Moreno, L. C., de la Cruz, W., & Teheran, P. (1994). *Thin Solid Films*,

- 252(1), 61–66. [https://doi.org/https://doi.org/10.1016/0040-6090\(94\)90826-5](https://doi.org/https://doi.org/10.1016/0040-6090(94)90826-5)
- Ishizaki, T., Saito, N., & Takai, O. (2009). *Journal of The Electrochemical Society*, 156(10), D413. <https://doi.org/10.1149/1.3190161>
- Izaki, M., & Omi, T. (1997). *Journal of The Electrochemical Society*, 144(6), 1949. <https://doi.org/10.1149/1.1837727>
- Kafi, F. S. B., Wijesundera, R. P., & Siripala, W. (2020). *Physica Status Solidi (A)*, 2000330. <https://doi.org/10.1002/pssa.202000330>
- Khallaf, H., Chen, C.-T., Chang, L.-B., Lupan, O., Dutta, A., Heinrich, H., Haque, F., del Barco, E., & Chow, L. (2012). *Applied Surface Science*, 258(16), 6069–6074. <https://doi.org/https://doi.org/10.1016/j.apsusc.2012.03.004>
- Kim, S., Lee, H., Park, C. M., & Jung, Y. (2012). *Journal of Nanoscience and Nanotechnology*, 12(2), 1616–1619. <https://doi.org/https://doi.org/10.1166/jnn.2012.4646>
- Lai, M., Gonzalez Martinez, J. A., Grätzel, M., & Riley, D. J. (2006). *Journal of Materials Chemistry*, 16(27), 2843–2845. <https://doi.org/10.1039/B606433G>
- Li, L., Liu, J., Su, Y., Li, G., Chen, X., Qiu, X., & Yan, T. (2009). *Nanotechnology*, 20(15), 155706. <https://doi.org/10.1088/0957-4484/20/15/155706>
- Park, H.-H., Park, H.-H., & Hill, R. H. (2006). *Sensors and Actuators A: Physical*, 132(2), 429–433. <https://doi.org/https://doi.org/10.1016/j.sna.2006.02.030>
- Pauporté, T., & Lincot, D. (2001). *Journal of Electroanalytical Chemistry*, 517(1), 54–62. [https://doi.org/https://doi.org/10.1016/S0022-0728\(01\)00674-X](https://doi.org/https://doi.org/10.1016/S0022-0728(01)00674-X)
- Peulon, S., & Lincot, D. (1998). *Journal of The Electrochemical Society*, 145(3), 864. <https://doi.org/10.1149/1.1838359>
- Riahi, I., Khalfallah, B., & Chaabouni, F. (2021). *Solid State Communications*, 340, 114487. <https://doi.org/https://doi.org/10.1016/j.ssc.2021.114487>
- Spray, R. L., & Choi, K.-S. (2007). *Chemical Communications*, 35, 3655–3657. <https://doi.org/10.1039/B704428C>
- Supothina, S. (2003). *Sensors and Actuators B: Chemical*, 93(1), 526–530. [https://doi.org/https://doi.org/10.1016/S0925-4005\(03\)00178-3](https://doi.org/https://doi.org/10.1016/S0925-4005(03)00178-3)
- Therese, G. H. A., & Kamath, P. V. (2000). *Chemistry of Materials*, 12(5), 1195–1204. <https://doi.org/10.1021/cm990447a>
- Vequizo, J. J. M., Wang, J., & Ichimura, M. (2010). *Japanese Journal of Applied Physics*, 49(12R), 125502. <https://doi.org/10.1143/JJAP.49.125502>
- Xiong, L., Guo, Y., Wen, J., Liu, H., Yang, G., Qin, P., & Fang, G. (2018). *Advanced Functional Materials*, 28(35), 1802757. <https://doi.org/https://doi.org/10.1002/adfm.201802757>